Int. J. Heat Mass Transfer. Vol. 14, pp. 1079–1091. Pergamon Press 1971. Printed in Great Britain

THE HETEROGENEOUS CONDENSATION OF MERCURY FROM A HIGH VELOCITY CARRIER GAS

J. J. MARKOWSKY and H. N. McMANUS, JR.

Sibley School of Mechanical Engineering, Cornell University, Ithaca, New York, U.S.A.

(*Received* 29 *July* 1970 *and in revised form* 13 *October* 1970)

Abstract—An analytical study of the condensation characteristics of mercury onto a cesium substrate in a nitrogen carrier gas was made. Good quantitative agreement was indicated between theory and experimental data [9] for heterogeneous condensation. A one-dimensional flow model was formulated, based on two-phase, three component gas dynamics, non-continuum growth relations and reaction heat term due to Cs–Hg amalgam formation. The results indicate that neglecting reaction heat, mass removal effects are dominant in the temperature range of this study. Substrate concentration was shown to have a direct effect on the magnitude of heterogeneous condensation. The effects of changing stagnation parameters on data presentation is considered.

NOMENCLATURE

A,	nozzle area [ft^2];
C_{pg},	specific heat a constant pressure of a gas component [Btu/lb$_m$°R];
C,	a constant equalling the total number of clusters of molecules in a particular distribution;
Cs,	symbol for cesium;
g_c,	dimensional constant [32·17 lb$_m$ft/lb$_f$s^2];
ΔG_f^*,	total change in Gibbs free energy in creating a condensed cluster of f critical sized molecules from the supersaturated vapor [Btu];
$\Delta G_f^{*\prime}$,	total change in Gibbs free energy related to the macroscopic point of view [Btu];
h,	enthalpy [Btu/lb$_m$];
h_{fg},	latent heat of vaporization, evaluated at the vapor temperature [Btu/lb$_m$];
H,	heat of reaction of amalgam [Btu/lb$_m$];
Hg,	symbol for mercury;
I,	dimensional constant [778·16 ft lb$_f$/lb$_m$Btu];
J,	nucleation rate per unit volume [nuclei/ft^3 s];
K,	Boltzmann's gas constant;
m,	mass flow rate [lb$_m$/s];
M,	molecular weight [lb$_m$/lbmole];
M_x,	Mach number (stream velocity/acoustic velocity);
$\dot{N}$,	nucleation rate [nuclei/s];
P,	pressure [lb$_f$/ft^2];
R,	universal gas constant [1545·3 ft lb$_f$/lb$_m$mole°R];
r,	droplet radius [ft];
T,	temperature [°R];
t,	time [s];
U,	flow velocity [ft/s];
V_L	liquid drop volume [ft^3];
x,	distance along nozzle axis [ft];
α,	mass of molecule [lb$_m$];
Γ,	gasification correction factor;
γ,	specific heat ratio;
ε,	mass accommodation coefficient (assumed equal to 0·50);
λ,	heating effect parameter due to condensation ($h_{fg}/C_{pg}T_g$);
μ,	ratio of mass of condensate to mass of mixture;

ρ,	density [lb_m/ft];
σ,	surface tension of liquid phase [lb_f/ft];
ϕ,	ratio of mass of amalgam to mass of mixture (m_a/m).

Subscripts

a,	refers to amalgam;
g,	refers to gas phase;
i, j,	refer to counting index or nozzle location;
L,	refers to liquid phase;
n,	refers to nitrogen gas;
0,	refers to plenum condition;
s,	refers to constant entropy;
V,	refers to vapor phase;
1,	refers to cesium;
2,	refers to mercury;
∞s,	refers to flat-film equilibrium state (saturated).

Superscripts

$*$,	refers to critical droplet size;
L,	refers to local property;
$'$,	refers to localized property, i.e. $(\ )/(\ )^L$.

A. INTRODUCTION

THE STUDY of the condensation of metals from the vapor state has been in progress for some time. Knowledge of this type is needed in evaluation of proposed power cycles for space applications. These studies have been concerned mainly with pure vapors and in general have been analytical rather than experimental.

An interesting class of problems involving condensation of metals from a gas mixture has been generated by the proposed gas core nuclear rocket. In this type unit the condensation and consequent recovery of a reactant is critical. In studying the efficiency of reactant recovery experimentally it is desirable to work with cheaper less hazardous materials. A fluid which suggests itself is mercury. The main detracting features of mercury are its toxicity and its reluctance to condense homogeneously. Precautions can be taken regarding toxicity. This study is concerned with overcoming the reluctance of mercury to condense rapidly by using heterogeneous condensation. By use of a suitable substrate material large quantities of mercury can be condensed in the time scale of a rapid expansion nozzle.

1. *Literature review*

The literature on condensation contains much work concerned with homogeneous nucleation [1–4]. This body of theory has been used to predict condensation characteristics of steam, and steam–gas mixtures [5–8]. The results obtained in these latter works suggest that the presently accepted nucleation theory is adequate for engineering predictions.

Reports of work with metal vapors are relatively few. McManus [9] has reported on the condensation characteristics of rubidium and cesium in a carrier gas both from an analytic and experimental viewpoint. This work also presented experimental results for mercury condensing on rubidium or cesium. Hill [10] and Griffin [11] have computed characteristics of metals, e.g. zinc, copper, rubidium, condensing from the pure vapor. It appears that no work concerned with the deliberate heterogeneous condensation of metal vapors from a carrier gas has been reported on other than the experimental results of [9].

B. THE ANALYTICAL MODEL

The thermodynamics system under consideration is a complex one. Physically an element of fluid is passing through a convergent–divergent nozzle. In so doing it experiences a sequence of processes. These are:

(1) A one-dimensional adiabatic single phase expansion;

(2) a nucleation of the homogeneously condensible species following supersaturation:

(3) growth of the stable nuclei formed by deposition of the homogeneously condensible species and/or the heterogeneously condensible species following its supersaturation, and

(4) an expansion of a two phase, i.e. gas and droplet fluid having identical velocities. In steps two and three large quantities of heat can be released with a consequent effect upon the expansion. In the case under consideration, mercury condensing on an alkali substrate, the possibility of heat addition from chemical reaction, amalgam formation, must be considered. The time scale of the complete expansion is of the order of 3×10^{-4} s.

1. *Flow conservation equations*

Consideration of the control volume of Fig. 1 leads to the continuity and momentum equation. The energy equation considers a unit mass of mixture. Second order terms have been neglected.

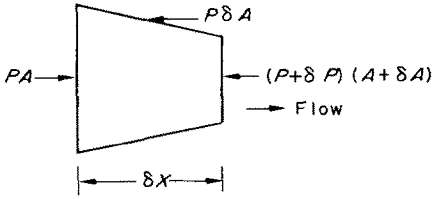

FIG. 1. Control volume.

Hence:

Continuity:

$$O = \frac{\mathrm{d}}{\mathrm{d}x}[\rho_n A_g U + \rho_{V1} A_g U + \rho_{V2} A_g U + \rho_{L1} A_{L1} U + \rho_{L2} A_{L2} U] \quad (1)$$

Momentum:

$$O = g_c A \frac{\mathrm{d}P}{\mathrm{d}x} + \frac{\mathrm{d}}{\mathrm{d}x}[m_n U + m_{V1} U + m_{V2} U + m_{L1} U + m_{L2} U] \quad (2)$$

Energy:

$$O = \frac{\mathrm{d}}{\mathrm{d}x}\left[m \frac{U^2}{I2g_c} + m_n h_n + m_{V1} h_{V1} + m_{V2} h_{V2} + m_{L1} h_{L1} + m_{L2} h_{L2}\right]. \quad (3)$$

To a good approximation

$$\rho_n = \frac{P_n M_n}{RT_g}, \qquad \rho_{V2} = \frac{P_{V2} M_{V2}}{RT_g}, \qquad \rho_{V1} = \frac{P_{V1} M_{V1}}{RT_g} \quad (4)$$

and the average density is given by

$$\rho_g = \frac{PM_g}{RT_g},$$

$$\rho_L = \frac{m_{L1}}{m_{L1} + m_{L2}} \rho_{L1} + \frac{m_{L2}}{m_{L1} + m_{L2}} \rho_{L2} \quad (5)$$

where

$$M_g = \frac{P_n}{P} M_n + \frac{P_{V1}}{P} M_{V1} + \frac{P_{V2}}{P} M_{V2}.$$

The continuity equation may be rewritten by integrating (1) and setting the integration constant equal to the total mass flow rate.

$$m = m_n + m_{V1} + m_{V2} + m_{L1} + m_{L2} = m_g + m_L \quad (6)$$

where

$$m_g = m_n + m_{V1} + m_{V2} = \rho_g A_g U$$

$$m_L = m_{L1} + m_{L2} = \rho_L A_L U.$$

Dividing (6) by m, setting $m_L/m = \mu$, and assuming $A = A_g$ or $A_L \ll A_g$ solve for m

$$m = \frac{\rho_g A U}{1 - \mu} \quad (7)$$

where

$$\mu = \mu_1 + \mu_2.$$

Differentiating (7) gives the specific continuity equation for two-phase three component flow

$$\frac{1}{\mathrm{d}x}\left[\frac{\mathrm{d}\rho_g}{\rho_g} + \frac{\mathrm{d}A}{A} + \frac{\mathrm{d}U}{U} + \frac{\mathrm{d}\mu_1}{1-\mu} + \frac{\mathrm{d}\mu_2}{1-\mu}\right] = 0. \quad (8)$$

Rewriting (2) by using (6) the momentum equation becomes

$$-g_c A \frac{\mathrm{d}P}{\mathrm{d}x} = m \frac{\mathrm{d}U}{\mathrm{d}x}. \quad (9)$$

The energy equation (3) may be transformed to a more usable form by introducing

$$h_L = h_V - h_{fg} - H$$

where the term $C_{pL}(T_V - T_L)$ has been dropped since T_L was set equal to T_g because of the effective heat removal characteristics of the noncondensable carrier gas, i.e. the number of molecules striking a droplet and incapable of condensing but capable of removing energy to those capable of condensing and adding energy is about 350 to 1. Also a heat of reaction term was introduced due to the possible formation of amalgams of mercury and cesium. The magnitude of H will be positive for heat liberated and negative for heat absorbed.

Substituting and rewriting the energy equation becomes

$$C_{pg}\frac{\mathrm{d}T_g}{\mathrm{d}x} + \frac{U}{Ig_c}\frac{\mathrm{d}U}{\mathrm{d}x} = h_{fg1}\frac{\mathrm{d}\mu_1}{\mathrm{d}x} + h_{fg2}\frac{\mathrm{d}\mu_2}{\mathrm{d}x} + H\frac{\mathrm{d}\phi}{\mathrm{d}x} \qquad (10)$$

where

$$\phi = m_a/m \text{ and } C_{pg} = \frac{m_n}{m}C_{pn} + \frac{m_V + m_L}{m}C_{pV}.$$

The terms $\mu \mathrm{d}h_{fg}$ and $\phi \mathrm{d}H$ were dropped because they are several orders of magnitude lower than those remaining.

2. *Nucleation equation*

The classical liquid nucleation theory was employed in order to evaluate the number of substrate droplets formed per unit time and volume. This may be written as

$$J = C\exp\left[-\Delta G_f^*/KT_g\right]. \qquad (11)$$

Currently, the above relationship has become controversial due to the ΔG_f^* term, which ignores the free energies of translation and rotation of the nuclei [1]. Due to the logarithmic nature of the term in question, the various points of view lead to great differences in the magnitude of J.

In equation form, the controversy entails rewriting ΔG_f^* to include the microscopic effects of the individual nuclei

$$\Delta G_f^* = \Delta G_f^{*\prime} - KT_g \ln \Gamma. \qquad (12)$$

Hence (11) becomes

$$J = C\Gamma \exp\left[-\Delta G_f^{*\prime}/KT_g\right] \qquad (13)$$

where "Γ", is commonly called the "gasification" correction factor, which takes into account the thermodynamic properties of the substrate nuclei which classical nucleation theory ignores.

In this study, the decision to use classical theory, i.e. $\Gamma = 1$ and $\Delta G_f^{*\prime} = \Delta G_f^*$ was due to lack of data on values for Γ and also because several prior works [9–11] have found good agreement between theory and experiment using classical theory for pure metal vapor condensation.

The entire expression for J has been rederived in [12] and only the final result is presented here.

$$J = \left(\frac{P_{V1}}{KT_g}\right)^2 V_{L1}\left(\frac{2\sigma_1}{\pi\alpha_1}\right)^{\frac{1}{2}} \exp\left[-\frac{4\pi\sigma_1(r_1{}^*)^2}{3KT_g}\right] \qquad (14)$$

where

$$r_1^* = 2\sigma_1 M_1/\rho_{L1} R T_g \ln\left(P_{V1}/P_{s\infty 1}\right). \qquad (15)$$

3. *Droplet conservation equations*

Droplet growth in itself is complex. To facilitate treatment the following simplifications have been introduced. Droplets do not interact or shatter. Because of the high thermal conductivity and the probability of liquid motion, i.e. mixing, droplet temperatures are considered uniform. Molecular velocity distributions are accurately described by the Maxwellian and gas diffusion gradients are negligible. It is probable that a diffusion limit on droplet growth would be confined to the latter phase of the condensation process. Thermal accommodation coefficients are taken to be unity.

Under these restrictions, the relation for the conservation of mass for a control volume containing a droplet is

$$\rho_L 4\pi r^2 \frac{dr}{dt} = \frac{4\pi r^2 \varepsilon}{\sqrt{(2\pi R T_g)}} \times [P_{V1}(\sqrt{M_1}) + P_{V2}(\sqrt{M_2}) - P_{L1}(\sqrt{M_1}) - P_{L2}(\sqrt{M_2})] \quad (16)$$

or noting that $dr/dt = U\,dr/dx$, and assuming $\varepsilon = 0{\cdot}50$, (16) becomes

$$\frac{dr}{dx} = \frac{1}{2\rho_L U \sqrt{(2\pi R T_g)}} [(P_{V1} - P_{L1})(\sqrt{M_1}) + (P_{V2} - P_{L2})(\sqrt{M_2})] \quad (17)$$

where $P_L = P_{s\infty} \exp(2\sigma M_L/\rho_L R T_g r)$, is the expression for the vapor pressure of a spherical drop having a radius "r". Also $P_V(\sqrt{M}/\sqrt{(2\pi R T_g)})$ is the number of particles striking a unit drop surface in unit time.

With the expression for the nucleation rate and drop growth rate, the relation for the condensation ratio can be determined by calculation of the condensation in an increment dx_j on each of the groups of drops formed during previous increment dx_i and also due to nucleation of particles in increment dx_j.

The nucleation rate in each increment dx_i is

$$\dot{N}_i = J_i A_i dx_i.$$

Thus, the condensate ratio can be written in differential form as

$$d\mu_{j1} = \frac{4\pi\rho_{L1}}{3m} \sum_{i=1}^{j-1} [\dot{N}_j r_{ij}^3 + 3\dot{N}_i r_{ij}^2 dr_{ij1}] \quad (18)$$

and

$$d\mu_{j2} = \begin{cases} \dfrac{4\pi\rho_{L2}}{3m} \displaystyle\sum_{i=1}^{j} \dot{N}_i r_{ij}^2 dr_{ij2} & \text{if } r_{ij} \geqslant 1{\cdot}3 r_{jj2}^* \\ 0 & \text{if } r_{ij} < 1{\cdot}3 r_{jj2}^*. \end{cases} \quad (19)$$

The size of substrate nuclei which have a probability of growth near unity, i.e. $r_{jj}^* = 1{\cdot}3\, r_j^*$, is given below for substrate and mercury condensation

$$r_{jj1}^* = (1{\cdot}3) 2\sigma_1 M_1/\rho_{L1} R T_g \ln(P_{V1}/P_{s\infty 1}) \quad (20)$$

$$r_{jj2}^* = (1{\cdot}3) 2\sigma_2 M_2/\rho_{L2} R T_g \ln(P_{V2}/P_{s\infty 2}). \quad (21)$$

The differential increment in droplet growth is

$$dr_{ij1} = \frac{dx_j(\sqrt{M_1})}{2\sqrt{(2\pi R T_g)} U_j \rho_{L1}} [P_{V1} - P_{L1}] \quad (22)$$

$$dr_{ij2} = \frac{dx_j(\sqrt{M_2})}{2\sqrt{(2\pi R T_g)} U_j \rho_{L2}} [P_{V2} - P_{L2}] \quad (23)$$

and, the drop size distribution at nozzle position "x_j" is given by

$$r_{ij} = r_{i,\,j-1} + dr_{ij1} + dr_{ij2}. \quad (24)$$

4. *Numerical solution of the equations*

The gas dynamic equations obtained from the three conservation equations, i.e. (8)–(10) are:

$$\frac{1}{P}\frac{dP}{dx} = \gamma_g M_x^2 \left[\left(\lambda_1 - \frac{1}{1-\mu}\right)\frac{d\mu_1}{dx} + \left(\lambda_2 - \frac{1}{1-\mu}\right)\frac{d\mu_2}{dx} + \frac{H}{C_{pg}T_g}\frac{d\phi}{dx} - \frac{1}{A}\frac{dA}{dx} \right] \Big/ [(M_x^2 - 1)(1-\mu) + \mu M_x^2 \gamma_g] \quad (25)$$

$$\frac{1}{T_g}\frac{dT_g}{dx} = \left(\frac{\gamma_g - 1}{\gamma_g}\right)(1-\mu)\frac{1}{P}\frac{dP}{dx} + \lambda_1 \frac{d\mu_1}{dx} + \lambda_2 \frac{d\mu_2}{dx} + \frac{H}{C_{pg}T_g}\frac{d\phi}{dx} \quad (26)$$

$$\frac{1}{U}\frac{dU}{dx} = -\frac{1}{\gamma_g M_x^2}\left(\frac{1}{P}\frac{dP}{dx}\right)(1-\mu). \quad (27)$$

Equations (18), (19) and (24)–(27) form a set which can be numerically solved for the pressure, temperature, velocity, droplet size, and mass fraction distribution.

The method of solution required:

(a) A nozzle contour (see Fig. 2)

(b) Restricting condensation to the supersonic portion of the nozzle.

(c) A criteria for estimating the onset of condensation was incorporated to decrease computing time. The criteria used was $J \geqslant 10^{19}$.

Property values were taken from [13]. Surface tension, a critical variable, was necessarily extrapolated by the method of Ramsay and Shield [9]. Because of the uncertainty of the extrapolation no correction for droplet surface curvature was made. Near the throat of the nozzle a transformation suggested by Glauz [14] was used to avoid the troublesome singularity. Restriction of condensation to the supersonic portion of the nozzle was necessary to reduce the throat problem to manageable proportions.

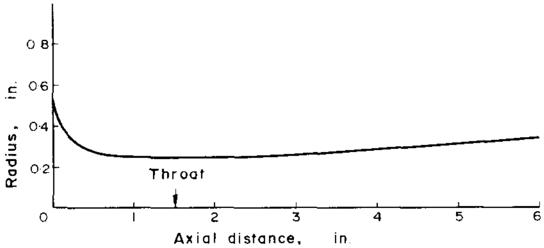

FIG. 2. Nozzle contour.

C. THEORETICAL RESULTS

1. *Homogeneous condensation*

To validate the analytical model, solutions were obtained for homogeneous condensation of cesium vapor in a nitrogen carrier gas. Conditions for these runs, i.e. runs 101 and 102, are given in Table 1. The restriction that condensation be confined to the supersonic portion of the nozzle proved unfortunate in that it prevented exact duplication of available experimental runs. While plenum temperature and pressure could be duplicated, use of equal partial pressures of Cs could cause condensation to initiate in the subsonic portion of the nozzle. Figure 3 presents the results of these runs.

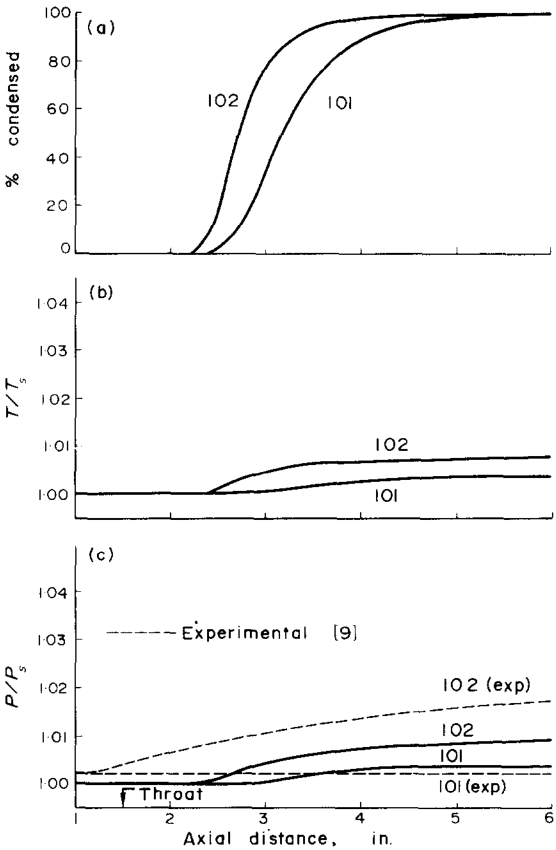

FIG. 3. Predicted pressure, temperature and fraction condensed for cesium.

The ordinates used in the pressure and temperature graphs are in actuality $(P/P_0)/$

Table 1. *Summary of initial flow conditions*

Run	Type of vapors	Plenum press (psia)	Plenum temp. (°R)	Theoretical alkali rate #/s	Exp. alkali rate #/s	Hg rate #/s	N_2 rate #/s	Total No. of drop formed
101	Cs	117·4	1180	$0{\cdot}481 \times 10^{-3}$	$1{\cdot}2 \times 10^{-3}$	—	0·4415	$2{\cdot}10 \times 10^{18}$
102	Cs	115·4	1255	$0{\cdot}115 \times 10^{-2}$	$0{\cdot}42 \times 10^{-2}$	—	0·4197	$1{\cdot}32 \times 10^{18}$
111	Cs–Hg	117·4	1180	$0{\cdot}464 \times 10^{-3}$	$0{\cdot}67 \times 10^{-3}$	0·04	0·4193	$2{\cdot}01 \times 10^{18}$
112	Cs–Hg	117·4	1180	$0{\cdot}464 \times 10^{-3}$	$0{\cdot}67 \times 10^{-3}$	0·04	0·4193	$2{\cdot}01 \times 10^{18}$
113	Cs–Hg	117·4	1180	$0{\cdot}347 \times 10^{-3}$	—	0·04	0·4194	$2{\cdot}56 \times 10^{18}$
114	Cs–Hg	117·4	1180	$0{\cdot}232 \times 10^{-3}$	—	0·04	0·4195	$3{\cdot}26 \times 10^{18}$

(P_s/P_0) and $(T/T_0)/(T_s/T_0)$ where P_0 and T_0 are the plenum quantities and P_s and T_s are the isentropic static quantities for a non-condensing, i.e. a fluid with the same physical properties as the condensing fluid, run. The plenum quantities being set equal cancel. It is well to note that the flows under consideration are not constant entropy, hence total pressure and total temperature vary axially. This will be commented on in a later section.

Examination of Fig. 3 and Table 1 indicates that parameter trends between experiment and analysis are in good agreement. No inconsistencies are evident between the two theoretical runs. It should be noted that the Mach number at which an increment of condensation takes place influences the pressure and temperature change noted.

The qualitative agreement between experiment and analysis and the internal consistency of the model is such as to increase confidence in its predictive abilities.

2. *Heterogeneous condensation*

Consideration of the governing equations indicate that several effects can occur simultaneously. These effects are mass removal, which is analogous to increased expansion ratio, heat addition due to phase change and heat addition caused by chemical reaction of substrate and condensible. The mass removal and phase change heat addition occur simultaneously in any condensation and oppose each other in overall effect. The chemical reaction is, of course, dependent on the species involved. In the present case, mercury and cesium do react with heat liberated.

As indicated, the model formulated has subscribed to the classical homogeneous nucleation theory. It has been contended by some, mainly in meteorological circles, that all condensation involves a heterogeneous mechanism. The present authors do not dispute the fact that nucleation sites, e.g. dust, etc., exist in any experimental system. However, in a rapid expansion nozzle for appreciable condensation to take place the number of sites necessary must be of the order predicted by homogeneous nucleation theory, i.e. approximately 10^{15} nuclei/ft^3 rather than that associated with dust, i.e. approximately 10^8 nuclei/ft^3. To an extent the present model allows evaluation of the relative importance of these effects.

2a. *Inert substrate nuclei.* Assigning a zero value to the reaction heat term is equivalent to having the Hg condense on an inert nuclei, e.g. dust, but in excess of 10^{15} nuclei per cubic foot. In Fig. 4, the results of such a run, i.e. run 111 is given. The pressure trace, Fig. 4c of run 111, gives comparison of an experimental Cs–Hg run and the equivalent inert substrate run, see Table 1.

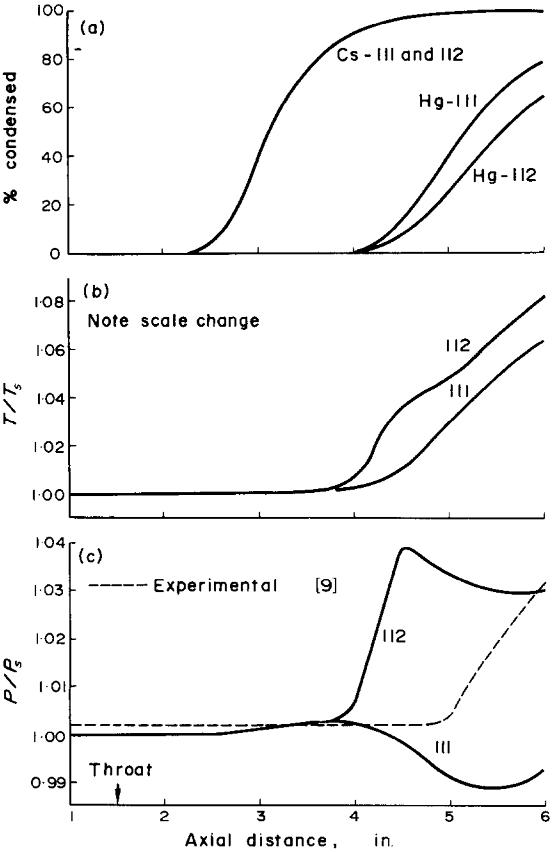

FIG. 4. Predicted pressure, temperature and fraction condensed for cesium–mercury. Run 111, reaction heat = 0 and run 112 reaction heat = 750 Btu/lb$_m$.

The difference is apparent. The anomalous behavior of the pressure plot illustrates that for an inert substrate the mass removal would dominate the opposing heat of condensation effect, in the temperature range encountered, i.e. 530°R, therefore, the pressure of the condensing run falls below that of an equivalent non-condensing run. From this it is safe to conclude that the dominant nuclei substrate is cesium with consequent reaction heat. A more extensive discussion of the opposing mass removal and heat of condensation effect are given in [12].

An examination of run 111 in Fig. 4a confirms the reluctance of mercury to condense even heterogeneously. In this run mercury reached saturation pressures $2\frac{1}{2}$ in. downstream of the inlet. However, no appreciable quantity of mercury is condensed until the four inch mark. The explanation for this lies in the critical drop size requirement for mercury to condense. In the interval between $2\frac{1}{2}$ and 4 in, cesium drops are growing but more importantly the required critical drop size for Hg condensation is falling rapidly with increasing supersaturation, see Fig. 6, run 112. The character of the condensation curves (Fig. 4a) for each species is similar. Homogeneous condensation of mercury was found to be of little importance in this system.

In Fig. 4c, run 111 emphasizes that the experimental results of Cs–Hg condensation is dominated by a heat liberation effect, i.e. an increasing pressure relative to a non-condensing run. The foregoing discussion has brought out that if heat of reaction is presumed zero, i.e. an inert substrate, then a completely contradictory behavior is predicted.

2b. *Reactive substrate material.* The heat of reaction would affect both the stream pressure and temperature equations. Although the heat of reaction of the cesium–mercury amalgams have not been experimentally determined, a theoretical approximation can be made in order to examine this effect. Pauling [15] has suggested the following relationship

$$H = 23\,\boldsymbol{Z}(E_1 - E_2)^2 \text{ kcal/g-mole}$$

where

$\boldsymbol{Z}$ = number of chemical bonds or valence link
E = electronegativity of the liquid metal

based on the close resemblance in the properties of the metallic and covalent bonds.

The composition of the amalgam formed was assumed to be Cs_2Hg, due to the stability of the outer electron orbitals of this compound. Using Pauling's theory, the numerical value of H is approximately 750 Btu/lb_m of amalgam.

The inclusion of the heat of reaction term had a radical effect on the pressure ratio plot and a lesser effect on the temperature ratio plot. These are shown by run 112 in Fig. 4.

The temperature ratio, run 112 of Fig. 4b, displayed an increased slope upon Hg condensation and then underwent another change due to the depletion of substrate, which terminated the formation of amalgam. The consideration of the heat of reaction increased the final temperature ratio, i.e. 1·082 vs. 1·063 for run 111.

The pressure ratio, run 112 of Fig. 4c, displayed a radically altered form. Rather than experiencing a drop in pressure upon start of Hg condensation a rapid rise occurs. This continues until all Cs has reacted at which point continued condensation results in a relative pressure decline.

The overshoot of pressure and steeper than experimental rise are attributable to ignoring of reaction and diffusion times. Heat of reaction additions were assumed to take place instantaneously upon condensation of Hg. In fact, a time lag would exist between deposition and liberation of heat. This lag would be caused mainly by the need for Hg to diffuse inward to contact unreacted Cs. As in the case of reaction heats there is no data dealing with diffusion and reaction rates. However, a time lag of about 5×10^{-5} s would be sufficient to bring the main portion of the theoretical results into good agreement with experiment. The overshoot portion of the pressure curve could be expected to be attenuated by increasing diffusion time required as droplet increased and because the heat added to the flow would be spread out over a finite time period instead of instantaneously. Consideration of these effects would be to smooth the theoretical curve. The estimated value of reaction heat appears reasonable since observed and predicted pressure rise are in good agreement.

2c. *Substrate concentration.* The effect of initial substrate concentration was investigated to determine its effect on the heterogeneous condensation. The substrate flow rates of runs 113 and 114 of Fig. 5 were 0·80 and 0·50 the value of run 112, respectively. Examining the results of runs 112, 113 and 114 in sequence, one notices the displacement and restriction of mercury condensation, due to the reduction of condensation sites. The mercury supersaturation ratios attained in runs 112, 113 and 114 were 6·1, 7·9 and 23, respectively, before condensation was indicated.

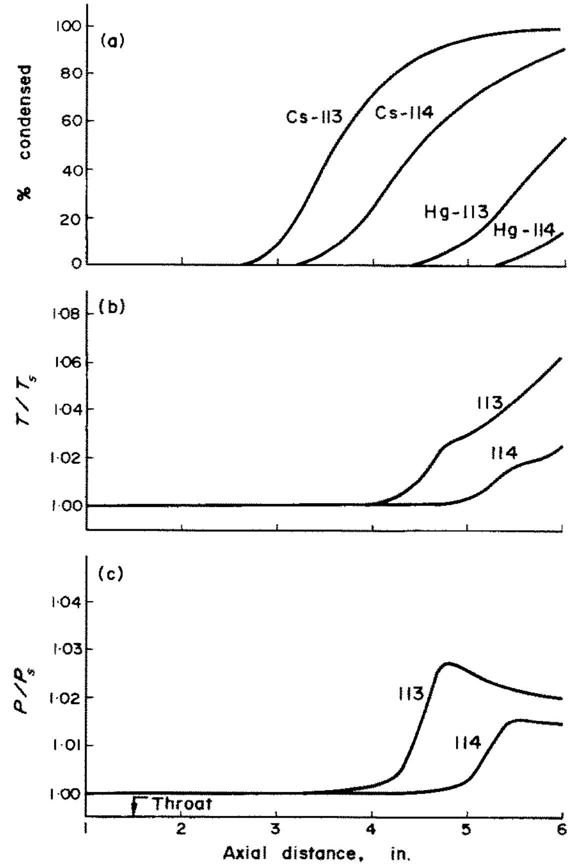

FIG. 5. Effect of substrate concentration on heterogeneous mercury condensation.

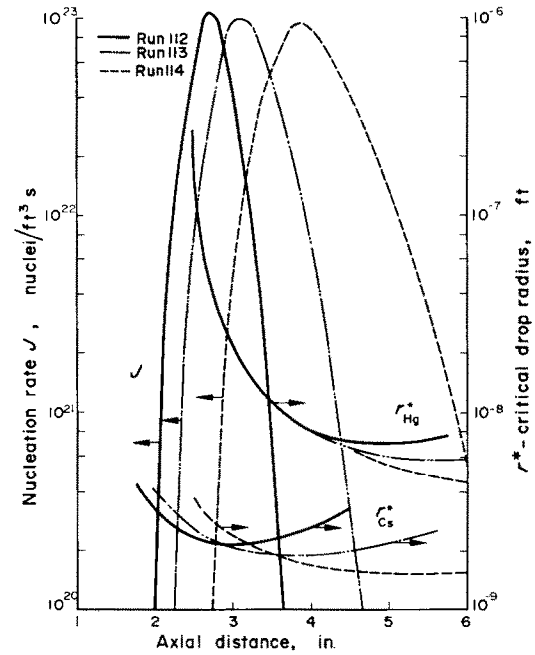

FIG. 6. Nucleation rate and critical drop size, runs 112, 113 and 114.

3. *Nucleation rates and critical drop size*

Figure 6 corresponding to data sets from runs 112, 113 and 114, indicates why condensation occurs only after an appreciable value of Hg supersaturation is reached. The critical drop size for Hg is inversely dependent on supersaturation. Therefore, the higher the supersaturation the smaller the critical drop size. The effect of substrate concentration is evident from Fig. 6. The larger substrate vapor pressure, i.e. run 112 promotes homogeneous growth rapidly and thus depletes the available substrate vapor and ends significant nucleation, i.e. $J < 10^{19}$ within 1¾ in. The data sets from runs 113 and 114 also in Fig. 6, indicate how substrate reduction delays homogeneous condensation and allows a longer time interval over which nucleation can occur. The longer-length interval for nucleation increases the total number of drops formed by 1·28 and 1·63 as many as for run 112. Although more drops were formed for lower substrate concentration, a reduction in mercury condensation indicated that the number of drops that were able to grow to meet the mercury critical size requirement decreased.

4. *Drop size distribution at the nozzle exit*

The four distributions plotted in Fig. 7 correspond to runs 101, 112, 113 and 114 which recorded 0, 15, 53 and 65 per cent of the initial mercury vapor condensed, respectively. The deviation of curve A from the homogeneous case, i.e. curve D, is because a portion of the substrate droplets have reached the critical size to accommodate mercury condensation. The distribution shown by curves B and C indicate that decreasing substrate concentration tends to yield a smaller number of smaller size drops with a consequent reduction in sites for Hg condensation. The displacements of the curves A, B and C from the homogeneous case are not as abrupt as one might expect due to the density difference, i.e. $\rho_{L1} = \frac{1}{8}\rho_{L2}$ and the cubic power relationship for mass addition onto a spherical drop.

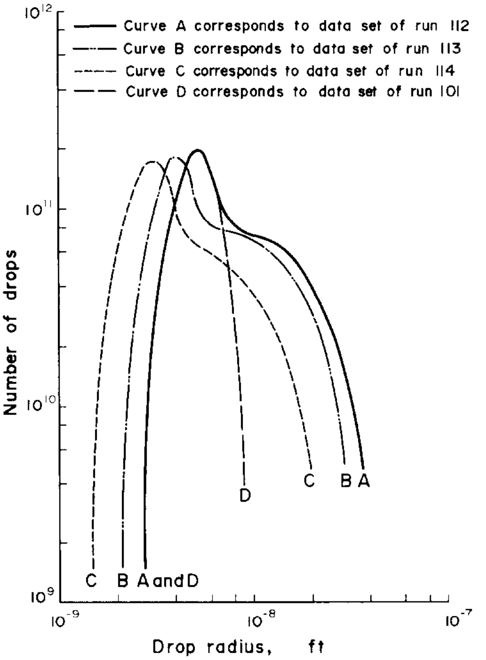

FIG. 7. Nozzle exit drop size distribution, runs 101, 112, 113 and 114.

5. *Non-constant stagnation*

The presentation of data has followed the practice of experiment, i.e. the measured static was referred to the plenum pressure. For an isentropic process the parameter is the ratio of static to total, and hence will give information concerning the Mach number. As indicated previously, the condensation phenomena is not isentropic and along the nozzle total temperature will rise and total pressure will fall.

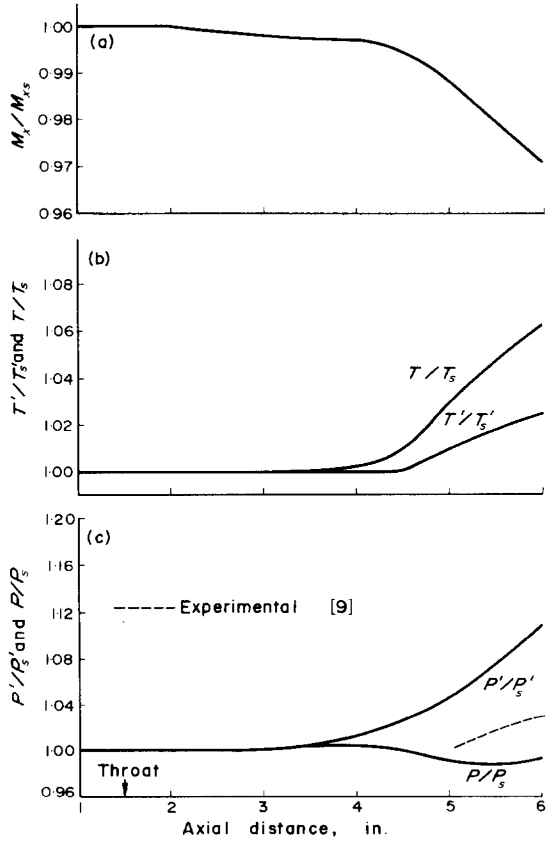

FIG. 8. Variation of flow parameters. Non-conserved total pressure and temperature considered, run 111, reaction heat = 0.

Figures 8a and 9a present the Mach number ratio, i.e. Mach number condensing/Mach number non-condensing, through the nozzle. As expected with condensation, the Mach number is reduced. In Figs. 8b and 9b, the parameter T'/T'_s describes the variation of total temperature, where $T'/T'_s = (T/T_0^L)/(T_s/T_0)$. As expected, the total temperature ratio increases which is shown by the fact that its values are below those of T/T_s. The total pressure ratio is seen to decrease as expected, since the values of P'/P'_s are greater than those of P/P_s. It should be recalled that Fig. 8 treats a Cs–Hg run where the heat of reaction is taken to be zero.

Figure 10 presents values of the ratio of static pressure to local total pressure. The isentropic total pressure is, of course, equivalent to plenum pressure. This form of presentation shows the difference between isentropic and non-isentropic to be of the order of 15 per cent.

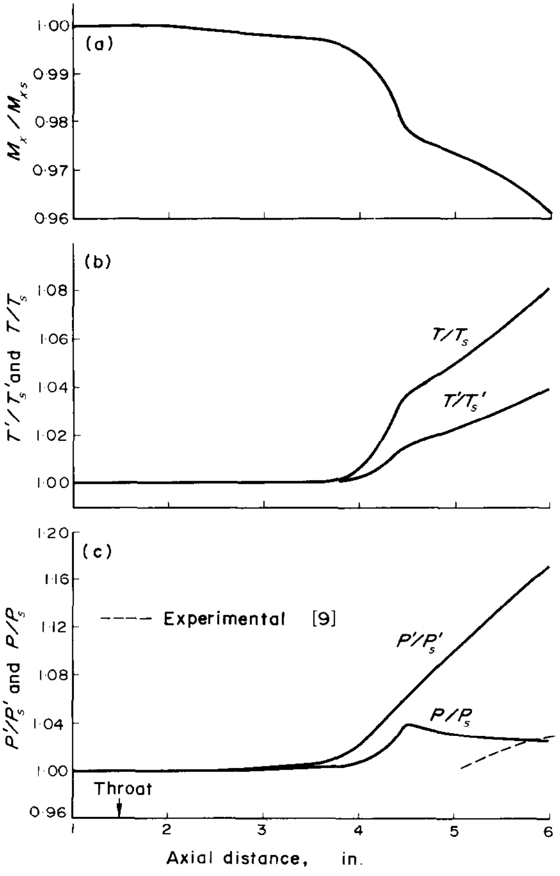

FIG. 9. Variation of flow parameters. Non-conserved total pressure and temperature considered, run 112, reaction heat = 750 Btu/lb_m.

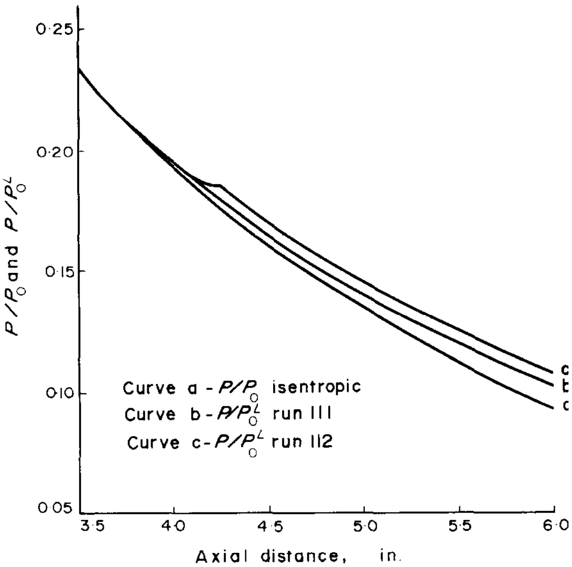

FIG. 10. Variation of pressure ratio with non-constant total pressure considered.

D. SUMMARY AND CONCLUSIONS

1. The extension of the growth equations to include Cs–Hg condensation necessitated the introduction of a reaction heat term due to amalgam formation. The introduction of the reaction heat term had the following effects: eliminated the predominance of mass removal associated with inert nuclei runs, enhanced agreement between theory and experimental data, indicated a shift and overshoot of the pressure ratio plot due to the computing method which did not incorporate the time lag from chemical reaction and heat diffusion.

2. The effect of decreasing substrate concentration was shown to retard heterogeneous condensation. Although Fig. 6 indicated a decrease in the difference between critical drop size, the time for homogeneous growth was reduced so that although more drops were

nucleated, the number that met mercury critical size requirement were reduced.

3. The drop sizes resulting from heterogeneous condensation were consistent with the kinetic theory assumption used in developing the growth relations, i.e. the droplet diameters were several orders of magnitude less than the mean free path which varied from 10^{-6} ft at the onset of condensation to approximately 10^{-5} ft at the exit of the nozzle.

4. The incorporation of non-constant stagnation properties was shown to have a non-trivial effect on data presentation. This was of the order of 15 per cent and 10 per cent for the data sets with and without the reaction heat term, respectively.

REFERENCES

1. G. M. Pound, J. Lothe, K. C. Russel and J. Fredev, Homogeneous nucleation and growth of droplets in vapors, *Adv. Phys.* **15**, 112–177 (1966).
2. J. Frenkel, *Kinetic Theory of Liquids*, pp. 366–400. Clarendon Press, Oxford, (1956).
3. H. G. Stever, Condensation in high speed flows, *High Speed Aerodynamics and Jet Propulsion*, Vol. III, pp. 526–573. Princeton Univ. Press, Princeton, N.J., (1958).
4. P. P. Wegener and L. M. Mack, Condensation in supersonic and hypersonic wind tunnels, *Adv. Appl. Mech.* V, 304–477 (1958).
5. A. M. Binnie and M. W. Woods, The pressure distribution in a convergent–divergent steam nozzle, *Proc. Inst. Mech. Engrs* **138**, 229–266 (1937).
6. A. M. Binnie and T. R. Green, An electrical detector of condensation in high velocity stream, *Proc. R. Soc.* **181A**, 134 (1942).
7. J. I. Yellot and C. K. Holland, The condensation of flowing steam, *Trans. Am. Soc. Mech. Engrs* **59**, 185 (1937).
8. P. G. Hill, Condensation of water vapor during supersonic expansion in nozzles, *J. Fluid Mech.* **25**, 593–620 (1966).
9. H. N. McManus, Jr., Condensation of metal vapor in a carrier gas, *Proc. Int. Heat Transfer Conference, 3rd. Chicago*, Vol. 2, p. 306 (1966).
10. P. G. Hill, H. Witting and E. P. Demetri, Condensation of metal vapors during rapid expansions, ASME paper no. 62-WA-123 (1962).
11. J. L. Griffin, Digital computer analysis of condensation in highly expanding flows, A.R.L., 63–206 (November 1963).
12. J. J. Markowsky, An analytical study of mercury vapor condensation onto an alkali metal substrate in a nitrogen carrier gas during rapid expansion, M.S. Thesis, Cornell University (1970).
13. W. D. Weatherford, Jr., J. D. Tyler and P. M. Ku, Properties of inorganic working fluids and coolants for space applications, WADC Tech. Report, 59-598 (1959).
14. R. D. Glauz, Combined subsonic-supersonic gas-particle glow, ARS Preprint, pp. 1717–61 (1961).
15. Linus Pauling, *The Nature of the Chemical Bond*, p. 92. Cornell U. Press, Ithaca, N.Y. (1960).

LA CONDENSATION HÉTÉROGÈNE DU MERCURE A PARTIR D'UN GAZ PORTEUR A GRANDE VITESSE

Résumé—On a fait une étude analytique des caractéristiques de la condensation sur un substrat de cesium, du mercure porté par un courant gazeux d'azote. Pour la condensation hétérogène, la théorie et les résultats expérimentaux sont en bon accord quantitatif. On a formulé un modèle d'écoulement monodimensionnel, basé sur deux phases; la dynamique des gaz à 3 composants, les relations de croissance non continue et le terme de chaleur de réaction dû à la formation de l'amalgame Cs–Hg. Les résultats indiquent qu'en négligeant la chaleur de réaction les effets de déplacement de masse sont dominants dans la gamme de température considérée dans cette étude. La concentration du substrat est montrée avoir un effet direct sur l'importance de la condensation hétérogène. On considère les effets de changement des paramètres de stagnation sur la présentation des résultats.

DIE HETEROGENE KONDENSATION VON QUECKSILBER AUS EINEM SCHNELLEN TRÄGERGAS

Zusammenfassung—Es wurde eine analytische Untersuchung angestellt über die charakteristischen Grössen der Kondensation von Quecksilber auf ein Cäsiumsubstrat mit Stickstoff als Trägergas. Für heterogene Kondensation wurde eine gute quantitative Übereinstimmung zwischen Theorie und experimentellen Werten [9] festgestellt. Es wurde ein eindimensionales Strömungsmodell aufgestellt, dàs aufbaut auf der Zwei-Phasen-, Drei-Komponenten-Gasdynamik, den Wachstumsgesetzen des Diskontinuums und dem

Term der Reaktionswärme bei der Bildung von Cs–Hg-Amalgam. Die Ergebnisse deuten an, dass bei Vernachlässigung der Reaktionswärme, Massentransporteffekte in dem untersuchten Temperaturbereich dominieren. Es zeigt sich, dass die Substratkonzentration einen direkten Einfluss auf die Grösse der heterogenen Kondensation hat. Der Einfluss der veränderlichen Parameter des Kesselzustands wird in der Darstellung der Daten berücksichtigt.

ГЕТЕРОГЕННАЯ КОНДЕНСАЦИЯ РТУТИ ИЗ ГАЗОВОГО ПОТОКА БОЛЬШОЙ СКОРОСТИ

Аннотация—Проведено аналитичекое исследование характеристик конденсации ртути на поверхность из цезия в потоке азота. Для гетерогенной конденсации получено хорошее количественное согласование между теорией и экспериментальными данными [9]. Сформулирована одномерная модель течения на основе газодинамики двухфазного трехкомпонентного течения, соотношений прерывного роста и теплоты реакции образования амальгамы Cs–Hg. Результаты показывают, что если пренебречь теплотой реакции, влияние отвода массы преобладает в исследуемом диапазоне температуры. Показано, что концентрация материала субстрата оказывает непосредственное влияние на скорость гетерогенной конденсации. Рассматривается влияние изменения параметров торможения.